RSC Advances

ROYAL SOCIETY
OF **CHEMISTRY**

www.rsc.org/advances

Journal Name

COMMUNICATION

Cesium Carbonate as surface modification material for organic-inorganic hybrid perovskite solar cells with enhanced performance

Haopeng Dong, Xudong Guo, Wenzhe Li and Liduo Wang*

Cs_2CO_3 has been employed as a new surface modification material for inorganic-organic hybrid perovskite solar cells. With the optimized modifying process, 14.2% power conversion efficiency (PCE) was got, enhancing nearly 20% compared with the control devices. Further studies showed that the PCE improvement mainly came from the retarded back recombination.

Though have been known for several decades, organic-inorganic hybrid perovskite materials $CH_3NH_3PbX_3$ (X=Cl Br I) have attracted great attention recently due to their huge success in photovoltage devices [1-3]. Since Miyasaka et.al. first reported 3.81% dye-sensitized solar cells with $CH_3NH_3PbI_3$ as light absorber in 2009, the conversion efficiency of solar cells based on hybrid perovskites has been surging[4]. The latest certified record published by NREL was 17.9%, got by Sang II Seok from KRICT. With the conversion efficiency improving fast, perovkiste solar cells' structure has also been evolved. Previous studies were all based on the structure of dye-sensitized solar cells, with a more or less 10 μm thick mesoporous TiO2 layer and I^-/I_3^- liquid electrolyte[5]. The instability of the devices due to the dissolution of the perovskites in the liquid electrolyte was a big challenge. By now, this problem was solved through replacing the liquid electrolyte with the solid hole transport materials (such as spiro-OMeTAD), and the thickness of mesoporous layer was also reduced to hundreds of nanometers, or even without the mesoporous layer[6-10].

Similar to dye-sensitized solar cells and organic solar cells, trap states at each layer's surface were easy to form charge-recombination centers[11]. Considering that perovskite layer itself had little deep traps, the situation of mesoporous TiO_2 surface became a key point for high conversion efficiency[12]. Surface modification with other materials was a useful method to passivate the TiO_2 surface traps and reduce the current loss resulting from the charge recombination[13]. Surface modification materials such as TiO_2, Al_2O_3, Y_2O_3, C_{60}, Graphene quantum dots and Sb_2S_3 had been reported[14-19]. Michael Gratel et.al studied using sub-nanometer conformal TiO_2

layer by atomic layer deposition as the blocking layer and 11.5% PCE was got[14].Shuzi Hayase et.al used Al_2O_3 or Y_2O_3 to passivate the mesoporous TiO_2 layer and after passivation with Y_2O_3, the efficiency increased from 6.59% to 7.5%[15].

Here we reported Cs_2CO_3 as a new surface modification material for perovskite solar cells. Cs_2CO_3 was widely used in organic light-emitting devices (OLEDs) to improve electron-injection from the metal cathod[20]. Our results showed that it could also act well in perovskite solar cells. Cs_2CO_3 had a work function of 2.2eV, much lower than TiO_2[21]. A thin Cs_2CO_3 layer between the mesoporoust-TiO_2/ $CH_3NH_3PbI_3$ interface would not affect the crystal of perovskite layer, but could reduce the charge recombination significantly. As a result, both the short-circuit current and fill factor of the photovoltaic devices improved, and the power conversion efficiency increased from 11.9% to 14.2%, giving a nearly 20% enhancement.

Perovskite solar cells were fabricated in the configuration mesoporous-TiO_2/ perovskite/ Spiro-OMeTAD/ Au. Detailed fabrication process could be found elsewhere[22]. For Cs_2CO_3 surface modification, 100 μl Cs_2CO_3/ DI water solution with certain concentration was dropped onto the sintered mesoporous-TiO_2 film (2.5cm*2.5cm), soaking for 30s, and then spinning at 2500rpm for 60s. The films were then sintered at 300°C for 30min before spinning the PbI_2 layer. Control devices were made under the same condition expect without the spinning of Cs_2CO_3 solution. We had tried to characterize the Cs_2CO_3 layer with TEM, but it seemed that it was too thin to be found. So we moved to XPS. As shown in Figure 1, XPS results clearly showed the existence of Cs. Considering that the decomposition temperature of Cs_2CO_3 was higher than 600°C, we thought this could indicate that the Cs_2CO_3 layer was introduced into the mesoporous TiO_2. The atomic ratio of films without and with Cs_2CO_3 surface modification tested by XPS could be found in Table S1 in the supporting information. To identify weather Cs_2CO_3 treatment had intermixing or doping effect to mp-TiO_2, we washed the modified mp-TiO_2 film softly with DI water for three times, and did XPS test again. The result could be found in Figure S1. Peaks from Cs_{3d} disappeared totally, showing that Cs_2CO_3 was washed out. That indicated that Cs_2CO_3 left in the
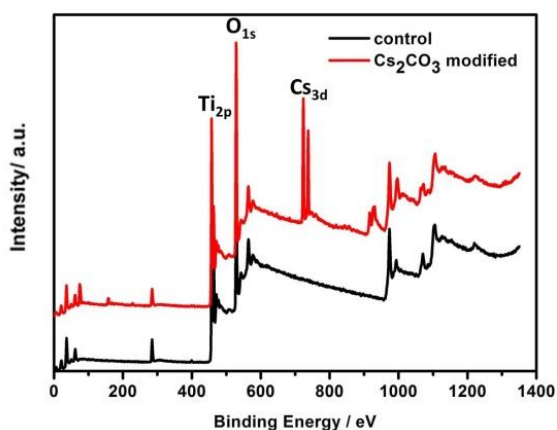
Figure 1. XPS results of films without and with Cs_2CO_3 surface modifiation

film formed only physical contact with mp-TiO_2 and should not affect the physical properties of mp-TiO_2. UV-vis absorption curves of the TiO_2 films without and with Cs_2CO_3 modified were shown in Figure 2. As expected, the absorption onset didn't change, indicating the bangap of the mp-TiO_2 hadn't changed after the Cs_2CO_3 modification.
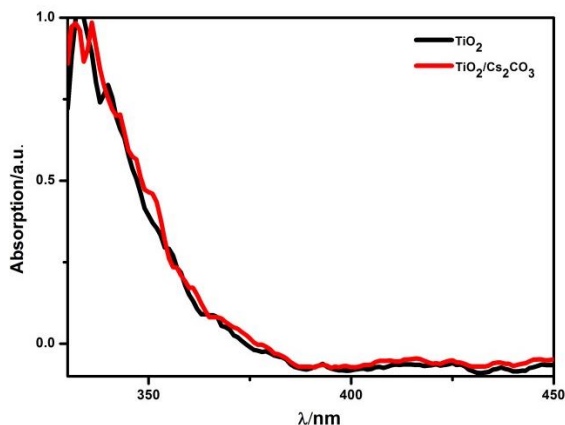

Figure 2. UV-vis absorption of TiO_2 films without and with Cs_2CO_3 modified.

In order to get the highest conversion efficiency, the thickness of the modification layer should be optimized. It could be easily controlled by adjusting the concentration of the solution used. Photovoltaic performance of devices modified with different Cs_2CO_3 concentration was shown in Table 1. Figure S2 illustrated the J-V curves of devices without and with Cs_2CO_3 modified using the optimized concentration (30mmol/L) under AM 1.5, 100mW/cm^2 solar irradiance. The results were got under reverse scan with a 50mV/s scanning speed, from 1.05V to 0V. J-V curves tested under different scanning directions were shown in Figure S3. There was a little difference for the forward and reverse scan, as noticed by others.[22] The reason for that still was not clear. We could see that, even with quite low concentration, Cs_2CO_3 modification gave a significant enhancement on the power conversion efficiency (PCE). J_{sc}, V_{oc} and FF were three key parameters that decided the final PCE. It was quite clear that Jsc increased regularly with increasing the Cs_2CO_3 concentration and started to decrease after reaching the optimized concentration (30mmol/L). This was not hard to understand because Cs_2CO_3 was a kind of insulating material; too thick Cs_2CO_3 layer would block the electrons' transport from perovskite into the mp-TiO_2. But when it was thin enough, electrons could pass through that with the tunnelling effect. This would be explained more detailed in the later discussion. V_{oc} also increased by

60eV from 0.97 V to 1.03V after Cs_2CO_3 modification. This improvement of V_{oc} was always found in the surface modification work of dye-sensitized solar cells and it was always attributed to the better passivated TiO_2 surface traps[24]. Different batches of devices were fabricated to make the results more convincing. Table S2(a) and (b) gave the parameters of one batch of devices.

Table 1. Photovoltaic parameters of perovskite solar cells modified with Cs_2CO_3 solution of different concentration

c_{Cs2CO3} / $mmol \cdot L^{-1}$	Voc/V	Jsc/mA$\cdot$ cm^{-2}	FF	PCE/%
0	0.97	19.8	0.62	11.9
5	0.95	20.3	0.68	13.2
15	0.96	20.7	0.68	13.5
30	1.03	21.3	0.65	14.2
45	1.02	19.1	0.68	13.3

To fully investigate possible reasons for the improved cell performance, we firstly checked weather the Cs_2CO_3 modification would affect the crystallization process of perovskite layer. Figure S4(a) and S4(b) showed the SEM results of perovskite layers without and with surface modification. In both cases, a compact perovskite capping layer was formed on the mesoporous TiO_2. No clear difference on the shape of the crystals was found, indicating that Cs_2CO_3 could not act with or get into the perovskite layer to affect its morphology. XRD was also done and the results were shown in Figure 3(a). In both cases, sharp diffraction peaks could be found at 14.1^o, 24.5^o, 28.4^o and 31.8^o, which were assigned as the (100), (111), (200), (210) lattice planes of the perovskite crystal, respectively. There were some changes on the relative peak intensities, showing that the crystallization of the perovskite changed after the Cs_2CO_3 surface modification. This might also affect the final performance of the devices and needed to be further researched. Peaks belonging to PbI_2 were also found in both films, indicating the incomplete conversion to perovskite. This was also noticed by others[25]. Considering the high PCE we got, the residual PbI_2 seemed to be not a trouble. Yang Yang et.al. recently even reported the formation of PbI_2 in the perovskite boundaries and at the relevant interface as the hole blocking layer for improved cells performance[26]. As expected, no peaks belonging to Cs_2CO_3 were found, consistent with the fact that Cs_2CO_3 layer for the surface modification was very thin. Figure 3(b) was the UV-vis absorption curves of the films without and with surface modification. After Cs_2CO_3 modification, the absorption of the perovskite film decreased slightly. This was because that after Cs_2CO_3 modification, Cs_2CO_3 filled into the pores in the mp-TiO_2, reducing the space left in the mp-TiO_2 film. As a result the total amount of perovskite was also reduced, leading to the decrease of absorption. But we could also notice that the absorption of the film was quite strong. Considering that we still had Au back contact that could act as a mirror to reflect the incident light, the perovskite film should be able to absorb nearly all the incident light. So this little decrease on the absorption would not affect largely on the final J_{sc}. Ultraviolet photoelectron spectroscopies (UPS) of the TiO_2/perovskite and TiO_2/Cs_2CO_3/perovskite were shown in the Figure S5. No peak position change was noticed, indicating that Cs_2CO_3 modification also hadn't led to the shift of the Fermi level and valence band position of the perovskite.
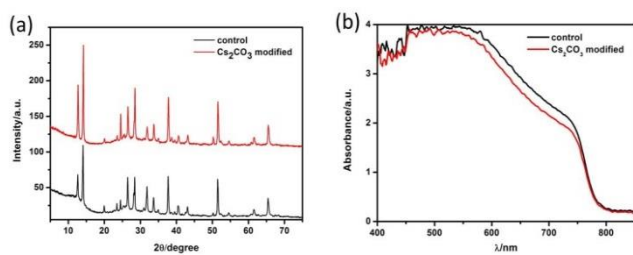
Figure 3. (a) XRD results and (b) UV-vis absorption results of the films without and with Cs_2CO_3 modification.

Now that the surface modification had not affect a lot on the morphology, crystallization and absorption of the perovskite layer, the performance improvement should be contributed to the internal physical changes. Figure 4(a) showed the *J-V* curves of devices without and with Cs_2CO_3 modification measured in dark. Compared with the control device, the onset of the dark current of surface modified device moved nearly 50 mV to higher voltage. This indicated that the back flow of electrons from TiO_2 to perovskite layer or the hole conductor was significantly suppressed. Considering that the electron recombination mainly happened due to the surface traps of the mesoporous TiO_2, the retarded dark current also showed that these surface traps were well passivated, which was in good agreement with the higher V_{oc} for surface modified devices.

Electrochemical impedance spectroscopy (EIS) was a simple but useful method to analyze the electron transport and interfacial properties inside the solar cells[27].Figure 4(b) showed the EIS results of devices measured in dark. Open-circuit voltage of the device was used as the bias for the testing. Due to the complexity arising from the mesoporous TiO_2 layer, only the middle frequency semicircles were found in the Nyquist plots, which presented the charge transfer resistance (R_{ct}) related to the recombination of electrons in TiO_2 with perovskite or hole transport layer. The larger the R_{ct} was, the less the electrons recombined at the surface. Figure 4(b) clearly showed that, after surface modification, the R_{ct} increased largely, which meant that the charge recombination was retarded, consistent with the conclusion from the dark *J-V* curves. This also explained the enhancement of the V_{oc}. Similar to the conventional solid-state DSCs, Gratzel et.al also noticed that in perovskite solar cells, the recombination rate increased when the quasi Fermi level of electrons in TiO_2 moved toward its conduction band[14]. Inversely, the retarded charge recombination meant the quasi Fermi level of n-type TiO_2 shifted up, leading to the increase of the device's V_{oc}. Figure 5 showed the incident photon to current efficiency (IPCE) curves for devices without and with Cs_2CO_3 surface modification. After the surface modification，IPCE increased in a large range, being consistent with the result the J_{sc} increased after the surface modification. In the range of 650-800nm, IPCE was nearly the same for both cases. We attributed this to the composite of the increased electron transport efficiency but decreased light harvesting efficiency.
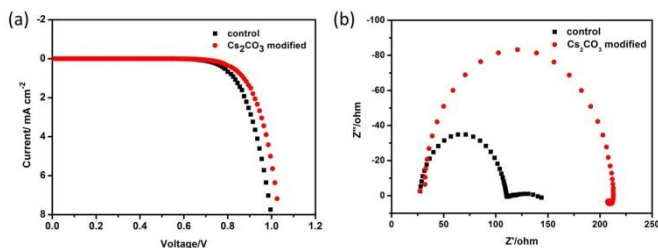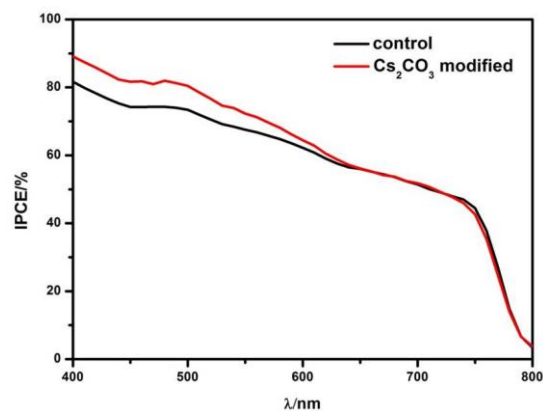

Figure 5. IPCE curves of devices without and with Cs_2CO_3 surface modification.

Combining with the above discussion, we gave a simple schematic diagram of the working principle of Cs_2CO_3 surface modification in Figure 6. After surface modification, a ultrathin insulating layer was introduced into the *mp*-TiO_2/$CH_3NH_3PbI_3$ interface. This ultrathin layer would not affect the forward electron transport, but could prevent the electrons in *mp*-TiO_2 from recombining with holes left in perovskite layer or in the hole transport layer (HTL). So that little current would loss during the electron transport process, giving an enhanced J_{sc}.
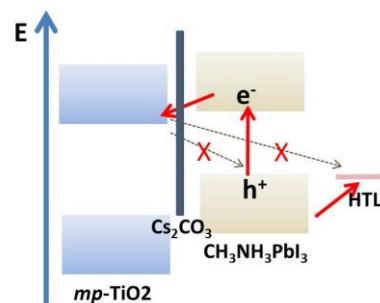

Figure 6. Schematic diagram of the working principle of Cs_2CO_3 surface modification.

In summary, we employed Cs_2CO_3 as the surface modification material for perovskite solar cells. Both the J_{sc} and V_{oc} enhanced after the surface modification. Further research showed that, the surface modification would not affect a lot on the crystal of the perovskite layer, but mainly contribute to the improved electron transport and retarded back recombination in the solar cells. With the optimized concentration, 14.2% conversion efficiency was finally got, increasing nearly 20% compared with the control devices.

Notes and references

Key Lab of Organic Optoelectronics and Molecular Engineering of Ministry of Education, Department of Chemistry, Tsinghua Uninversity, Beijing, P.R.China. E-mail: chldwang@mail.tsinghua.edu.cn

1. R.F. Service, *Science*, 2014, **344**, 458.
2. S. Kazim, M.K. Nazeeruddin, M. Gratzel and S. Ahmad, *Angew. Chem. Int. Ed.*, 2014, **53**, 2812.
3. T.C. Sum and N. Mathews, *Energy Environ. Sci.*, 2014, **7**, 2518.
4. A. Kojima, K. Teshima, Y. Shirai and T. Miyasaka, *J. Am. Chem. Soc.*, 2009, **131**, 6050.

Figure 4. (a) *J-V* curves of devices without and with Cs_2CO_3 surface modification tested in dark; (b) EIS cycles of devices tested in dark.

5. J.-H. Im, C.-R. Lee, J.-W. Lee, S.-W. Park and N.-G. Park, *Nanoscale*, 2011, **3**, 4088.

6. H.-S. Kim, C.-R. Lee, J.-H. Im, K.-B. Lee, T. Moehl, A. Marchioro, S.-J. Moon, R. Humphry-Baker, J.-H. Yum, J.E. Moser, M. Gratzel and N.-G. Park, *Scientific Reports*, 2012, **2**, 591.

7. M. M. Lee, J. Teuscher, T. Miyasaka, T.N. Murakami and H. J. Snaith, *Science*, 2012,**338**, 643.

8. J. Burschka, N. Pellet, S.-J. Moon, R. Humphry-Baker, P. Gao, M.K. Nazeeruddin and M. Gratzel, *Nature*, 2013, **499**, 316.

9. M. Liu, M.B. Johnston and H. J. Snaith, *Nature*, 2013, **501**, 395.

10. Q. Chen, H. Zhou, Z. Hong, S. Luo, H.-S. Duan, H.-H. Wang, Y. Liu, G. Li and Y. Yang, *J. Am. Chem. Soc.*, 2014, **136**, 622.

11. T. Leijtens, B. Lauber, G. E. Eperon, S. D. Stranks and H.J. Snaith, *J. Phys. Chem. Lett.*, 2014, **5**, 1096.

12. W.-J. Yin, T. Shi and Y. Yan, *Appl. Phys. Lett.,* 2014, **104**, 063903.

13. A.K. Chandiran, M.K. Nazeeruddin and M. Gratzel, *Adv. Funct. Mater.*, 2014, **24**, 1615.

14. A.K. Chandiran, A. Yella, M.T. Mayer, P. Gao, M.K. Nazeeruddin and M. Gratzel, *Adv. Mater.*, 2014, **26**, 4309.

15. Y. Ogomi, K. Kukihara, S. Qing, T. Toyoda, K. Yoshino, S. Pandey, H. Momose and S. Hayase, *ChemPhysChem*, 2014, **15**, 1062.

16. W. Li, J. Li, L. Wang, G. Niu, R. Gao and Y. Qiu, *J. Mater. Chem. A,* 2013, **1**, 11735.

17. A. Abrusci, S.D. Stranks, P. Docampo, H.-L. Yip, A.K. Jen and H.J. Snaith, *Nano Lett.*, 2013, **13**, 3124.

18. Z. Zhu, J. Ma, Z. Wang, C. Mu, Z. Fan, L. Du, Y. Bai, L. Fan, H. Yan, D.L. Phillips and S. Yang, *J. Am. Chem. Soc.*, 2014, **136**, 3760.

19. S. Ito, S. Tanaka, K. Manabe and H. Nishino, *J. Phys. Chem. C*, 2014, DOI: 10.1021/jp500449z

20. J. Huang, Z. Xu and Y. Yang, *Adv. Funct. Mater.*, 2007, **17**, 1966.

21. G. Li, C.W. Chu, V. Shrotriya, J. Huang and Y. Yang, *Appl. Phys. Lett.,* 2006, **88**, 253503.

22. W. Li, H. Dong, L. Wang, N. Li, X. Guo, J. Li and Y. Qiu, *J. Mater. Chem. A*, 2014, **2**, 13587.

23. N.J. Jeon, J.H. Noh, Y.C. Kim, W.S. Yang, S. Ryu and S.II, Seok, *Nature Mater.*, 2014, **13**, 897.

24. E. Palomares, J.N. Clifford, S.A. Haque, T. Lutz and J.R. Durrant, *J. Am. Chem. Soc.*, 2003, **125**, 475.

25. V. Somsongkul, F. Lang, A.R. Jeong, M. Rusu, M. Arunchaiya and T. Dittrich, *Phys. Status Solidi RRL*, 2014, DOI: 10.1002/pssr.201409292.

26. Q, Chen, H. Zhou, T.-B. Song, S.Luo, Z. Hong, H.-S. Duan, L. Dou, Y. Liu and Y. Yang, *Nano Lett*., 2014, **14**, 4158.

27. A. Dualeh, T. Moehl, N. Tetreault, J. Teuscher, P. Gao, M.K. Nazeeruddin and M. Gratzel, *ACS Nano*, 2014, **8**, 362.